Weldments: Metallographic Techniques and Microstructures

By Glenn S. Huppi, Research Engineer, Center for Welding Research, Colorado School of Mines; Brian K. Damkroger, Research Engineer, Center for Welding Research, Colorado School of Mines; Craig B. Dallam, Research Engineer, Center for Welding Research, Colorado School of Mines

<Previous section in this article

Atlas of Microstructures for Weldments

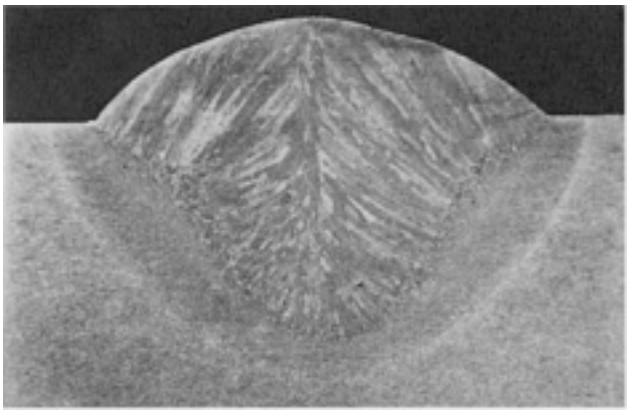

Fig. 5 19-mm (0.75-in.) A-710 steel plate, submerged arc weld. Heat input: 3.0 MJ/m. Macrostructure shows the fusion zone, heat-affected zone, and base metal in a single-pass, bead-on-plate weld. 85 mL H_2O + 15 mL HNO_3 + 5 mL methanol. 3.5×

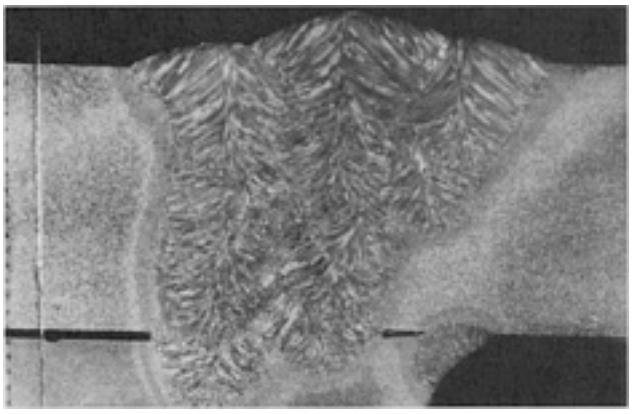

Fig. 6 Same as Fig. 5. Weld wire: 2.4 mm ($\frac{3}{32}$ in.). Mil Spec 100S-1, OP121TT flux. Heat input: 1.0 MJ/m. Macrostructure shows the fusion zone, heat-affected zone, reheat zones, and base metal in a multiple-pass butt weld. 85 mL H_2O + 15 mL HNO_3 + 5 mL methanol. 2×

Fig. 7 19-mm (0.75-in.) A-710 steel plate, submerged arc weld. Microstructure shows dragout of base metal scale between the base metal and the epoxy filler used in the gap between the base plate and backup plate in a multiple-pass butt weld. As-polished. 280×

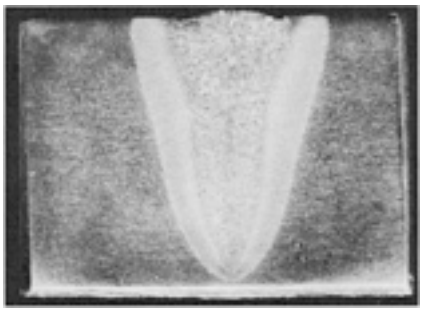

Fig. 8 2.25Cr-1Mo steel plate, single-pass electron beam weld. Heat input: 0.5 MJ/m. Macrostructure shows high depth-to-width ratio of the fusion zone, which is typical of high energy density welding processes. 85 mL H_2O + 15 mL HNO_3 + 5 mL methanol. 2.8×

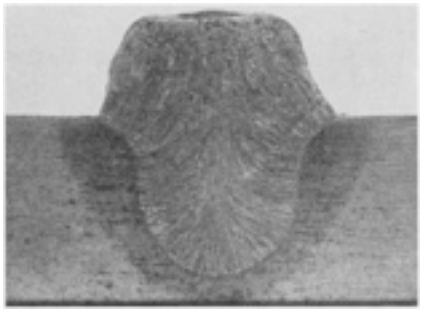

Fig. 9 13-mm (0.5-in.) Lukens Frostline steel plate, submerged arc weld. Heat input: 2.0 MJ/m. Weld wire: AWS E70S-3. Macrostructure shows unusual bead shape due to surface tension and viscosity abnormalities in a calcium-fluoride-base experimental fused flux. 85 mL H_2O + 15 mL HNO_3 + 5 mL methanol. 1.5×

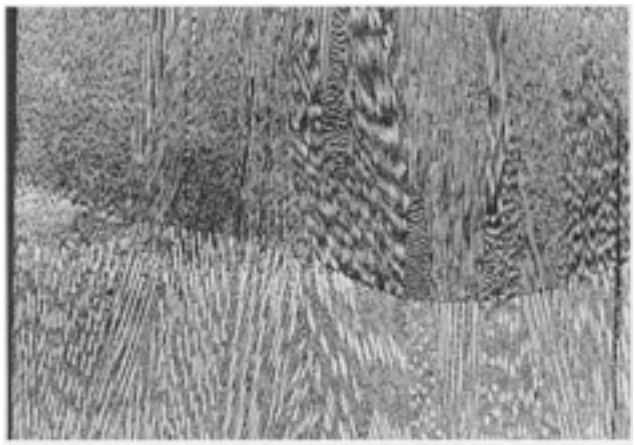

Fig. 10 25-mm (1.0-in.) type 304 stainless steel plate, shielded metal arc weld. Heat input: 1.0 MJ/m. Micrograph shows austenite-dendrite structure retained across successive weld passes in the fusion zone. 10% oxalic acid electroetch. 40×

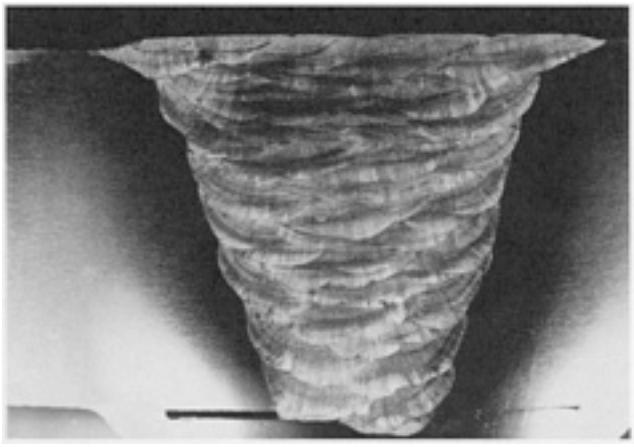

Fig. 11 25-mm (1.0-in.) type 304 stainless steel plate, shielded metal arc weld. Heat input: 1.0 MJ/m. Macrograph shows epitaxial grain growth resulting in continuous columnar grains occurring through successive passes in a multiple-pass weld. 10% oxalic acid electroetch. 2×

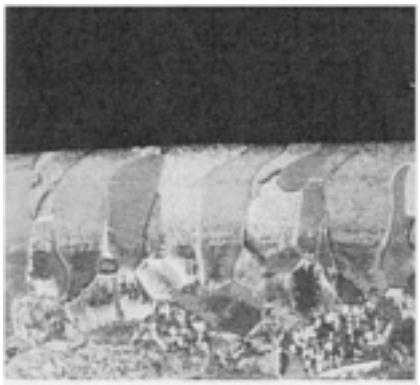

Fig. 12 13-mm (0.5-in.) Ti-6Al-2Nb-1Ta-1Mo alloy plate, autogenous single-pass gas tungsten arc weld. Heat input: 2.0 MJ/m. Longitudinal section showing curvature of the prior-β grains, which follow the maximum thermal gradient in the weld pool. 1:1 solution, Kroll's etch and distilled water. 3×

Fig. 13 13-mm (0.5-in.) Ti-6Al-4V alloy plate, autogenous two-pass gas tungsten arc weld. Heat input: 2.0 MJ/m. Weld was made over a groove in the base plate into which metallic yttrium had been pressed. Microstructure shows aligned yttrium oxide particles, indicating the segregation that occurred during solidification. 1:1 solution, Kroll's etch and distilled water. 100×

Fig. 14 13-mm (0.5-in.) AlS1 4340 steel plate, submerged arc weld. Heat input: 1.9 MJ/m. Fusion zone microstructure in which the dendrite solidification structure is revealed by the distribution of tempered martensite and upper bainite. 2% nital. 50×

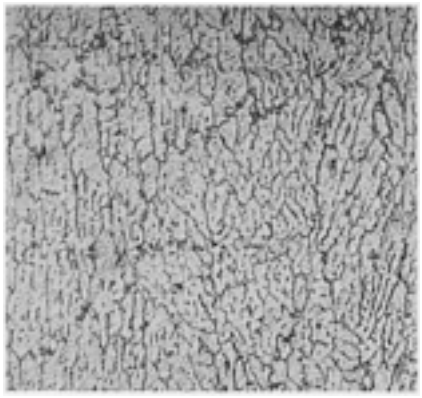

Fig. 15 2219 aluminum alloy, gas metal arc weld (parameters unknown). Fusion zone microstructure in which the cellular solidification structure is revealed by the distribution of the divorced eutectic microconstituent between the cells. Kroll's etch. 200×

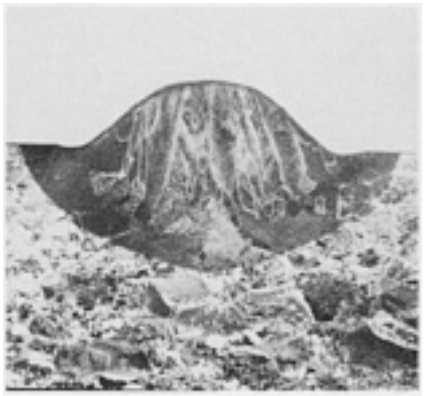

Fig. 16 13-mm (0.5-in.) Ti-6Al-2Nb-1Ta-1Mo alloy plate, single-pass gas metal arc weld. Heat input: 0.8 MJ/m. Macrograph showing the columnar prior-β grains resulting from epitaxial growth. 1:1 solution, Kroll's etch and distilled water. 4×

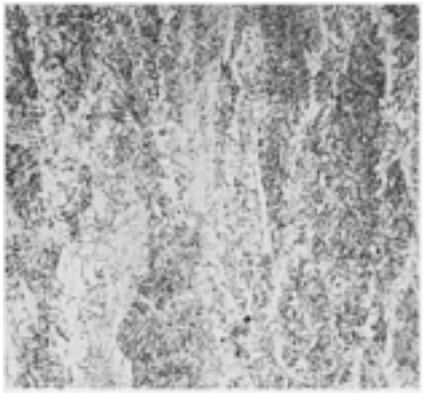

Fig. 17 16-mm ($\frac{5}{8}$-in.) A-36 steel plate, single-V butt multiple-pass shielded metal arc weld. Heat input: 1.3 MJ/m. Weld wire: AWS E7018. Low-carbon fusion zone microstructure showing veins of grain boundary ferrite on prior austenite grain boundaries. 2% nital. 50×

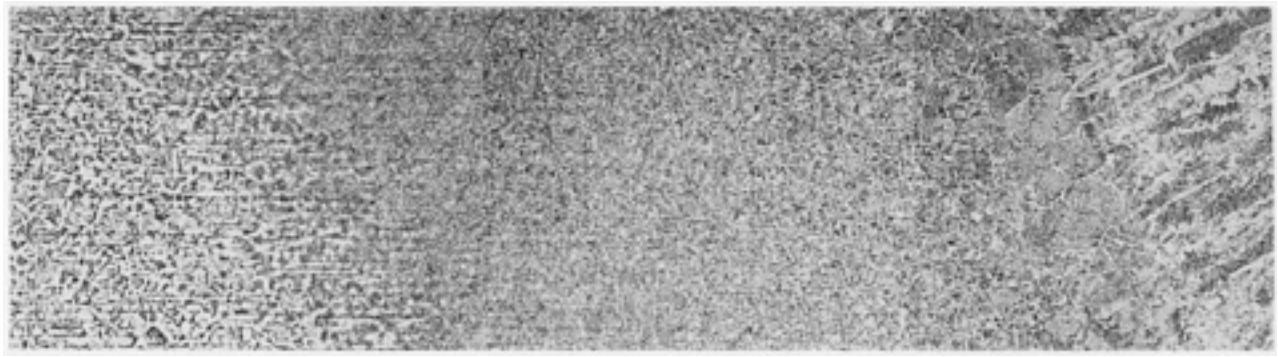

Fig. 18 16-mm ($\frac{5}{8}$-in.) A-36 steel plate, multiple-pass shielded metal arc weld. Heat input: 1.3 MJ/m. Composite micrograph of the heat-affected zone showing (from left to right) base plate, tempered zone, partially transformed zone, fine grain zone, coarse grain zone, fusion line, and fusion zone. 2% nital. 36×

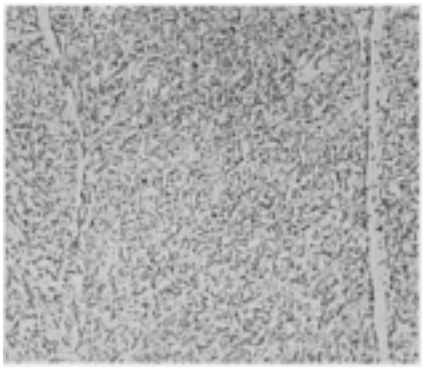

Fig. 19 19-mm (0.75-in.) A-710 steel plate, last pass (12th) of a submerged arc single-V butt weld. Heat input: 1.3 MJ/m. Grain boundary ferrite on prior austenite grain boundaries in a microstructure of fine acicular ferrite. 2% nital. 500×

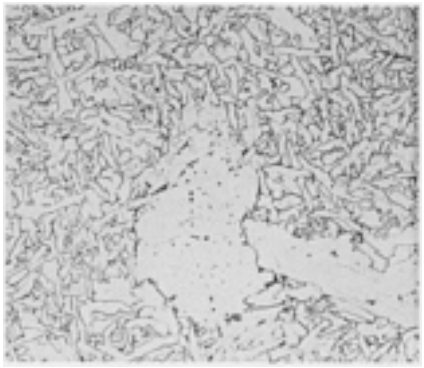

Fig. 20 16-mm ($\frac{5}{8}$-in.) A-36 steel plate, multiple-pass shielded metal arc single-V butt weld. Heat input: 1.3 MJ/m. Weld wire: AWS E7018. Fusion zone microstructure containing polygonal ferrite in coarse acicular ferrite. 2% nital. 500×

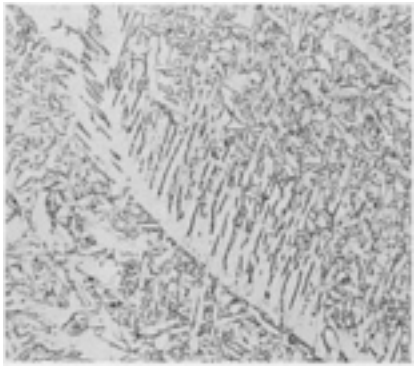

Fig. 21 13-mm (0.5-in.) Lukens Frostline steel plate, submerged arc bead-on-plate weld. Heat input: 1.9 MJ/m. Weld wire: AWS E70S-3. Fusion zone microstructure with Widmanstätten ferrite growth from grain boundary ferrite with coarse acicular ferrite. 2% nital. 500×

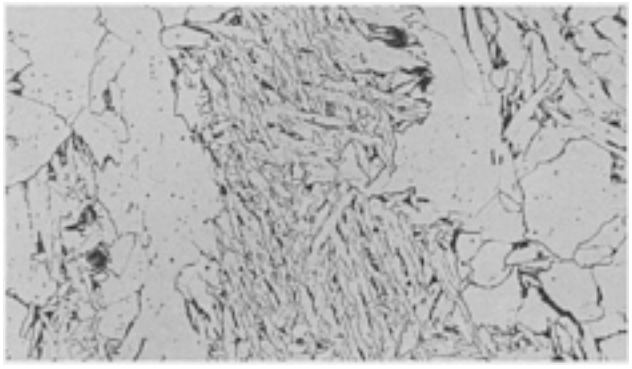

Fig. 22 16-mm ($\frac{5}{8}$-in.) A-36 steel plate, multiple-pass shielded metal arc single-V butt weld. Heat input: 1.3 MJ/m. Weld wire: AWS E7018. Fusion zone microstructure containing bainite and ferrite-carbide aggregate in coarse grain boundary ferrite. 2% nital. 500×

Fig. 23 13-mm (0.5-in.) Ti-6Al-4V alloy plate, autogenous single-pass gas tungsten arc weld. Heat input: 2.0 MJ/m. Fusion zone microstructure consisting of fine Widmanstätten α + β and grain boundary α. 1:1 solution, Kroll's etch and distilled water. 100×

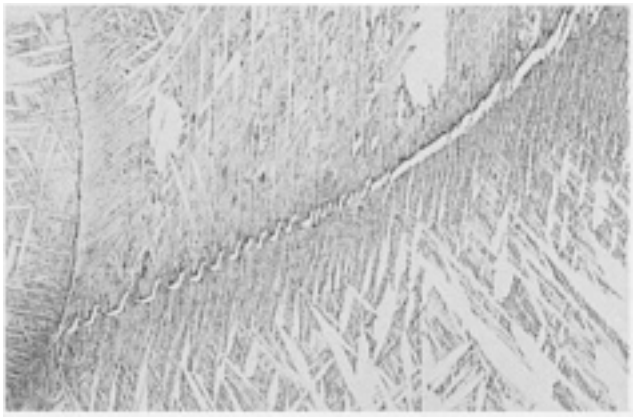

Fig. 24 13-mm (0.5-in.) Ti-6Al-2Nb-1Ta-1Mo alloy plate, autogenous single-pass gas tungsten arc weld. Heat input: 2.0 MJ/m. Fusion zone microstructure containing grain boundary α, α', massive α, and Widmanstätten α + β. 1:1 solution, Kroll's etch and distilled water. 400×

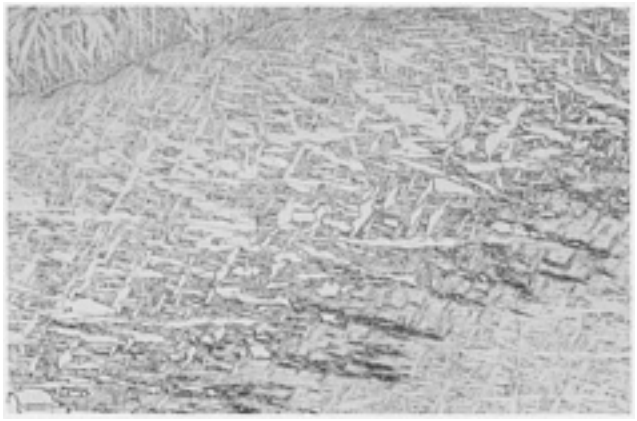

Fig. 25 13-mm (0.5-in.) Ti-6Al-2Nb-1Ta-1Mo alloy plate, three-pass gas metal arc weld. Heat input: 0.8 MJ/m. Reheat zone of the third pass showing α', Widmanstätten α + β, equiaxed α, and slightly higher amount of retained β than the areas surrounding the reheat zone. 1:1 solution, Kroll's etch and distilled water. 250×

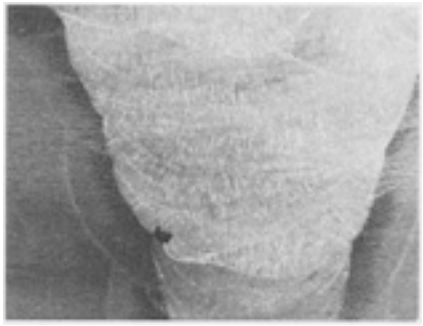

Fig. 26 38-mm (1.5-in.) HY 80 steel plate, gas shielded flux core weld. Heat input: 2.0 MJ/m. Macrosection revealing slag entrapment in a double-V buff weld. Use of etchants is helpful in locating such defects because residual etchant "bleeds out" of defect and stains adjacent areas. 2% nital. 3×

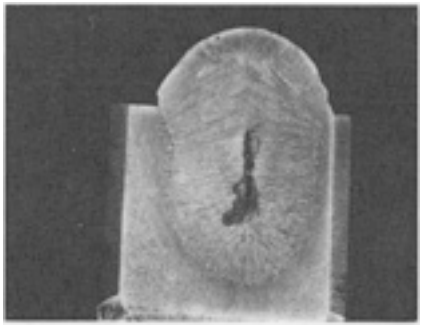

Fig. 27 13-mm (0.5-in.) AISI 4340 steel plate, submerged arc weld. Heat input: 1.9 MJ/ m. Macrograph shows solidification (centerline) cracking. Crack position is highlighted by etchant "bleed out." 85 mL H_2O + 15 mL HNO_3 + 5 mL methanol. 1.5×

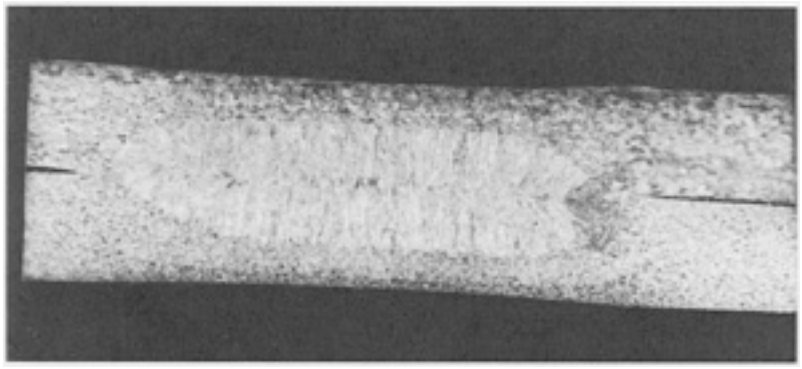

Fig. 28 Low-carbon hot-rolled sheet, resistance spot weld (composition and weld parameters unknown). Macrostructure shows 60% penetration of the weld and columnar growth pattern in the fusion zone. 85 mL H_2O + 15 mL HNO_3 + 5 mL methanol. 10×

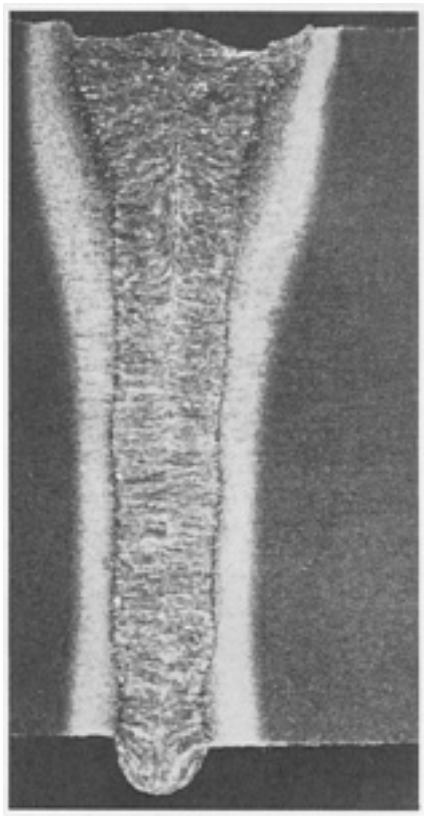

Fig. 29 14-mm ($\frac{9}{16}$-in.) A-710 steel plate, outagenous single-pass laser butt weld. Heat input: 0.014 MJ/m. Macrograph shows the high depth-to-width ratio of the weld bead and the limited size of the heat-affected zone. 2% nital. 8×

<Previous section in this article